New insights into the electrocatalytic mechanism of methanol oxidation on amorphous Ni-B-Co nanoparticles in alkaline media

Fanhua Wu[ab], Zhonglin Zhang[a], Fusheng Zhang[a], Donghong Duan[a], Yu Li[a], Guoqiang Wei[a], Shibin Liu [c,d]**, Qinbo Yuan [c,d]**, Enzhi Wang[c,d], Xiaogang Hao[a]

[a]*Department of Chemical Engineering, Taiyuan University of Technology, Taiyuan 030024, China*

[b]*School of Science, North University of China, Taiyuan 030051, China*

[c]*The State Key Laboratory of Hydroscience and Engineering of Tsinghua University, Beijing 100084, China*

[d]*Sanjiang yuan Coll aborative Innovation Center, Tsinghua University, Beijing 100084, China*

*Corresponding authors.

Tel.: +86-351-6018554; fax: +86-351-6018554. E-mail address: sbliu@tyut.edu.cn (S.B. Liu); qbyuan@tpeco.cn@qq.com (Q.B. Yuan)

EXPERIMENTAL

Physical characterization

The Ni-B and Ni-B-Co catalyst nanoparticles was characterized by a DX-2700 X-ray diffractometer (XRD) with Cu Kα radiation (λ = 0.154 nm, scan rates = 8° min^{-1}, 2θ = 5° -85°) at 40 kV and 30 mA, a Thermo Scientific ESCALAB 250Xi instrument (XPS) with Al Kα radiation (hv = 1486.6 eV) at 14.8 kV.

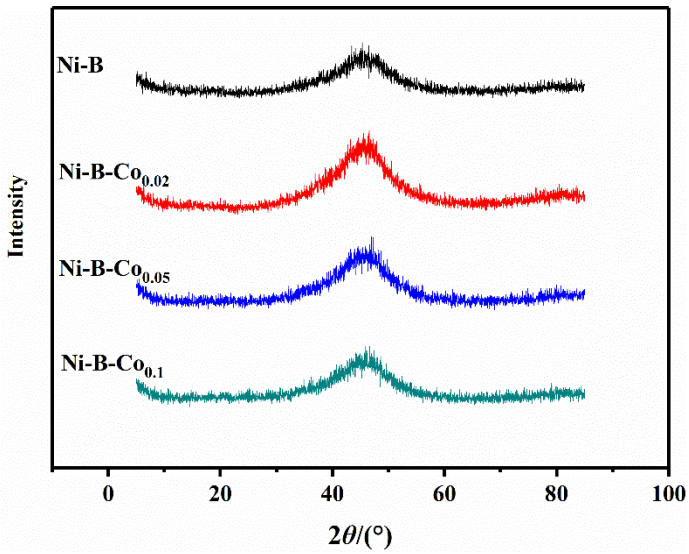

Figure S1. XRD patterns of Ni-B and Ni-B-Co nanoparticles

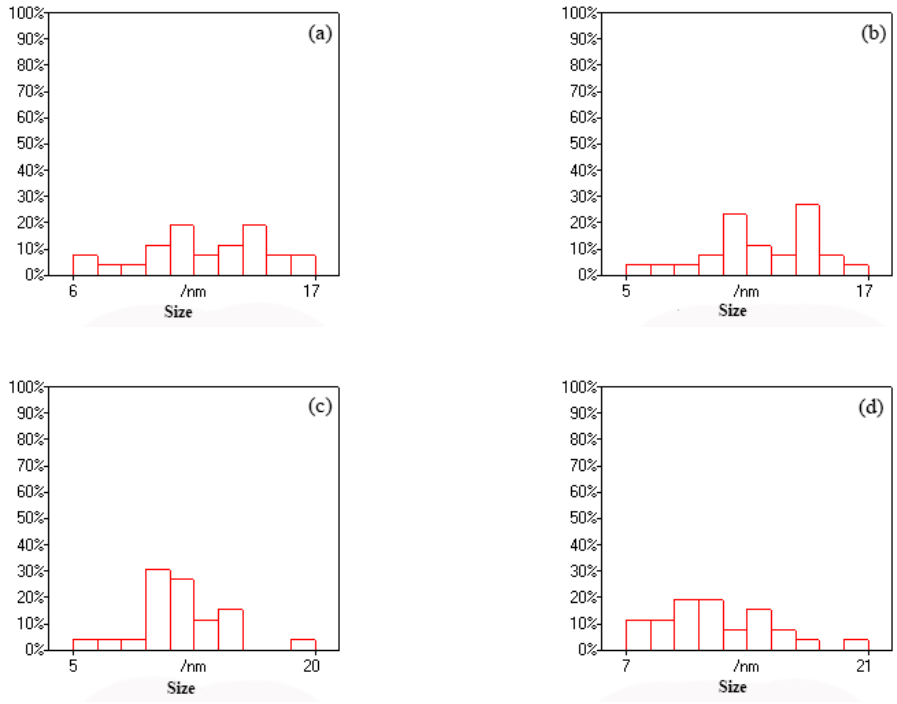

Figure S2. The particle size distribution histograms of Ni-B(a), Ni-B-$Co_{0.02}$(b), Ni-B-$Co_{0.05}$(c), and Ni-B-$Co_{0.1}$(d) nanoparticles from TEM

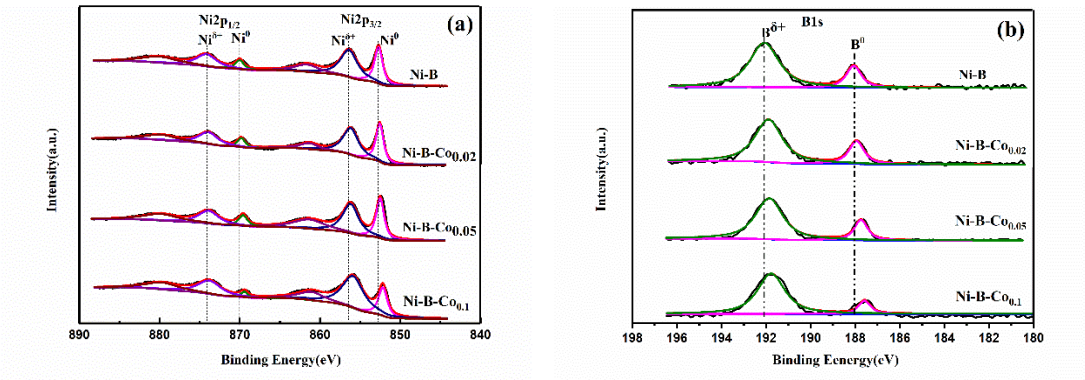

Figure S3. XPS spectra of Ni2p (a) and B1s (b) for Ni-B and Ni-Co-B nanoparticles

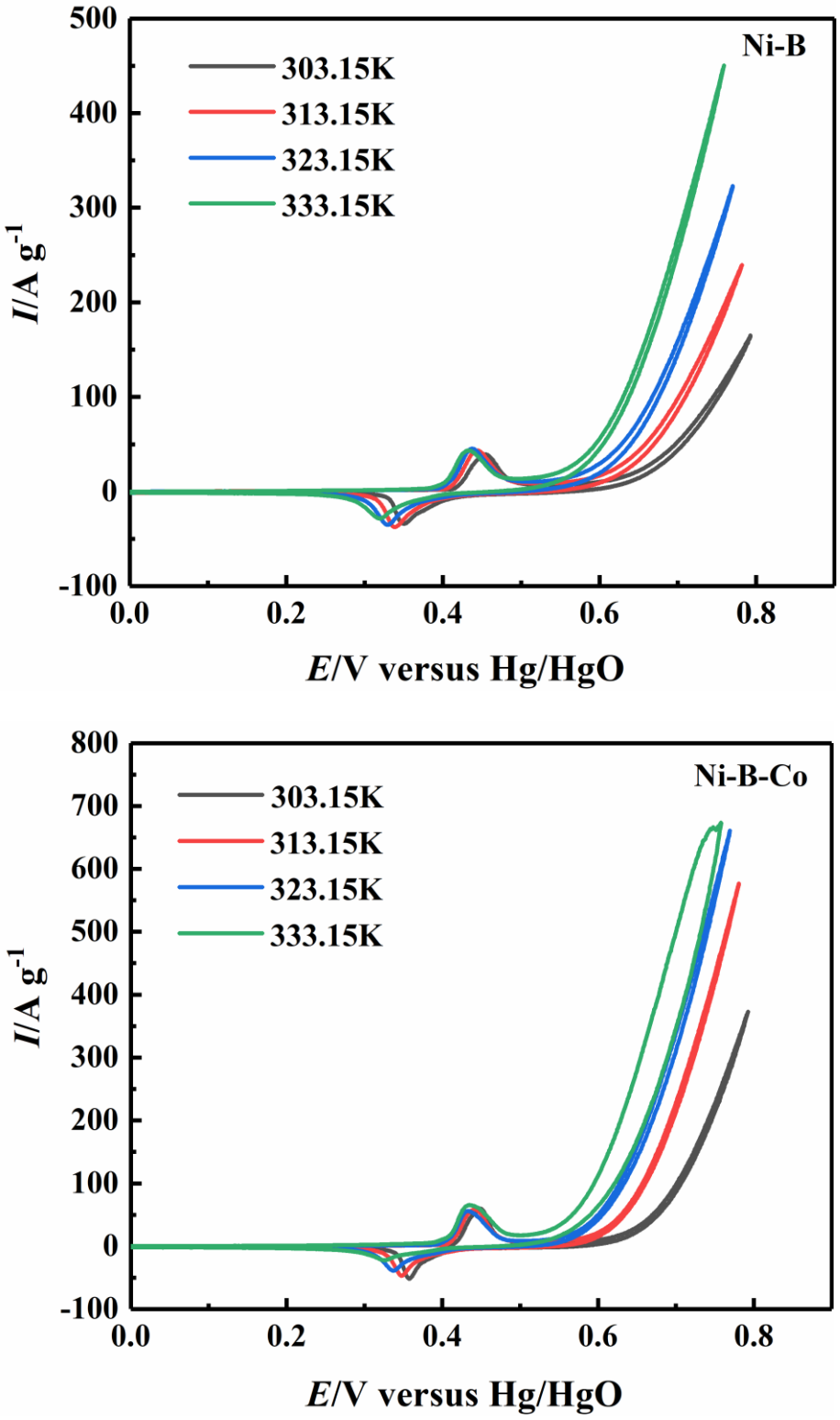

Figure S4. Cyclic voltammograms on Ni-B and Ni-B-$Co_{0.05}$ nanoparticles in a range from 0.0 to 0.8 V at different temperatures in 1 M NaOH solution

Table S1 The bulk and surface atomic ratios of Ni-B and Ni-B-Co nanoparticles

Sample	bulk atomic ratios (ICP)			surface atomic ratios (XPS)		
	Ni/at.%	B/at.%	Co/at.%	Ni/at.%	B/at.%	Co/at.%
Ni-B	62.73	37.27	0	46.44	53.56	0
Ni-B-$Co_{0.02}$	62.08	36.55	1.37	39.58	49.15	11.27
Ni-B-$Co_{0.05}$	59.28	37.60	3.12	46.25	48.01	5.73
Ni-B-$Co_{0.1}$	57.49	36.57	5.94	41.47	49.95	8.58